



Published in final edited form as:

Radiol Clin North Am. 2021 May ; 59(3): 349–362. doi:10.1016/j.rcl.2021.01.004.

Clinical applications of magnetic resonance spectroscopy (MRS) in of brain tumors: from diagnosis to treatment

Brent D. Weinberg, MD, PhD¹, Manohar Kuruva, MD¹, Hyunsuk Shim, PhD², Mark E. Mullins, MD, PhD¹

¹Department of Radiology and Imaging Sciences, Emory University, Atlanta, GA

²Department of Radiation Oncology, Emory University, Atlanta, GA

Keywords

brain tumor; glioblastoma; magnetic resonance spectroscopy; pseudoprogression; radiation necrosis; tumor progression

Introduction

Magnetic resonance spectroscopy (MRS) is a technique which combines the ability of nuclear magnetic resonance (NMR) to differentiate molecules with the imaging features of localization unique to magnetic resonance imaging (MRI). This provides a “molecular window” into the component chemistry of a given tissue, allowing for unique insight into physiologic or disease (pathophysiologic) processes. MRS requires no injected contrast agent and no ionizing radiation is involved, which are obvious safety benefits.

There are many applications of MRS to imaging of brain tumors which have been explored, some of which have already reached clinical practice and others which have been confined predominantly to research applications (Table 1). In clinical application, MRS can potentially differentiate primary brain tumors from other potential mimics, such as demyelinating disease, lymphoma, or infection. Additionally, the “molecular signatures” of high-grade and low-grade tumors often differ, allowing prediction of how aggressive a tumor may be. After treatment, MRS can provide insight into whether treated tissue consists predominantly of radiation necrosis or tumor, a considerable diagnostic dilemma. More research-oriented applications include surveying a tumor to locate the most aggressive area to target for biopsy and radiation therapy using high resolution whole brain spectroscopic MRI.

MRS has several limitations which have prevented it from reaching its full potential in brain tumor imaging. Despite the theoretical ability to differentiate tissues of different types, there is substantial overlap between the spectroscopic appearances of different diseases. MRS can be time consuming and highly variable between different imaging locations; moreover, artifacts often limit evaluation.

This work provides an overview of the use of MR spectroscopy in brain tumor imaging, including general imaging principles and technique, key imaged metabolites, the typical appearance of overlapping disease processes, and practical limitations on MRS. The second section discusses ongoing development of new applications likely to have an impact on clinical care in coming years.

Imaging Technique

Early in the development of NMR, it was discovered that nuclei in different molecular environments resonated at slightly different frequencies.¹ In simplest terms, when subjected to an applied magnetic field, molecules precess at a resonant frequency that varies with the surrounding molecular environment. This effect, known as chemical shift, allows nuclei in different chemical environments to be distinguished based on their resonant frequencies. A shielding parameter, defined in parts per million (ppm), describes the relative change compared to a reference compound. The shielding parameter is a constant, while the chemical shift measured in Hz increases linearly with field strength. As a result, the resolution of spectroscopy increases with increasing field strength.

Most imaging spectroscopy applications image the hydrogen nucleus (^1H) because it is the most prevalent nucleus in tissue. Spectroscopy of other elements is possible,² although not used widely in practice. For *in vitro* proton (^1H) spectroscopy, chemical shift values (δ) are reported in ppm relative to a tetramethylsilane (TMS). *In vivo*, compounds such as TMS are not available, so usually one of the indigenous spectral signals is used as a reference (e.g. for the brain, the N-acetyl resonance of N-acetylaspartate (NAA), set at 2.02 ppm, is often used).

Virtually all MRS studies are performed by collecting time domain data after application of either a 90° pulse, or an echo-type of sequence. The time domain signal is then converted to the frequency domain through Fourier transformation (FT), which allows the viewing of the signal intensity as a function of frequency (i.e., in the frequency domain). To accumulate sufficient signal to noise (SNR), the scan can be repeated many (N) times and averaged together to improve signal-to-noise-ratio, which is proportional to the \sqrt{N} . Choosing an appropriate N and scan repetition time (TR) is required to balance image acquisition time and optimize SNR.^{3,4} Successful ^1H MRS also requires water and lipid suppression techniques, since water and lipids are present at concentrations many-fold higher than target metabolites, which are usually present in the millimolar range. Magnetic field homogeneity and field strengths have to be sufficient to allow resolution of the relatively small chemical shift range of protons (~ 10 ppm). Large and/or membrane-associated molecules are not usually well-seen, although their broad resonances contribute to the baseline of the spectrum.⁵

The information from a brain MR spectrum depends on several factors, such as the field strength, echo time, and type of pulse sequence. On a 1.5T scanner with long echo times (TE) (e.g. 140 or 280ms), only choline (Cho), creatine (Cr), and N-acetyl aspartate (NAA) are typically observable in healthy adult brain, while compounds such as lactate, alanine, or others may be detectable if their concentrations are elevated above normal levels due to

abnormal metabolic processes.⁶⁻⁸ At short TE (≤ 35 ms), additional compounds including glutamate, glutamine, myo-inositol, lipids, and other macromolecules may become detectable.

Spatial localization allows signals to be recorded from well-defined structures or lesions within the brain.⁹⁻¹² In the 1980s, a wide range of spatial localization techniques were developed for *in vivo* spectroscopy;¹³ however, many were either difficult to implement, involved too many RF pulses, or were inefficient. Out of this plethora of sequences, two emerged as simple and robust enough for wider use, each based on three slice-selective pulses applied in orthogonal directions. The STEAM sequence (Stimulated Echo Acquisition Mode)¹⁴⁻¹⁷ uses three 90° pulses and detects the resulting stimulated echo from the volume intersected by all three pulses, while the PRESS sequence (Point REsolved Spectroscopy Sequence)^{18,19} uses one 90° pulse and two 180° pulses to detect a spin echo from the localized volume. The sequence is designed so that signals from other regions outside the desired voxel are eliminated (usually by using crusher gradients).^{14,20} Typical voxel sizes for brain ¹H MRS are approximately 8 cm³. Multi-voxel (2D, or 3D) PRESS MRSI sequences are available on commercial MR scanners from most scanner vendors and are the most commonly applied MRS technique.²¹

Metabolites

The most described metabolites in brain tumor spectroscopy are choline, N-acetyl aspartate, creatine, lipids, myo-inositol, and lactate (summarized in Table 2). A representative normal spectrum from the cerebral hemisphere is shown in Figure 1. The area under each curve represents the number of spins identified; however, this result is only quantitative if an external reference (of known concentration) is used. As such, the areas under the curve are usually evaluated in a relative fashion. Some systems automatically produce relative area under the curve numbers. In the absence of these numbers, peak height is often used as a surrogate marker. While alterations in the concentrations of these each metabolites can be seen with various pathologies, a combination of the relative changes of these various metabolites in conjunction with other imaging features can be useful in distinguishing primary brain tumors from metastases, grading gliomas, and distinguishing recurrence from radiation necrosis. Sometimes, ratios of metabolites (such as Cho/Cr, or Cho/NAA) can be used to increase the sensitivity of a particular measure. In practice, this is one of the most commonly used approaches.

Choline (Cho, 3.2 ppm) is a precursor of acetylcholine, a component of cell membranes. Elevated Cho is a marker of increased cell turnover which can be seen with tumors and other proliferative processes. In combination with other imaging features, elevated Cho can identify high cellular turnover pathologies like gliomas and lymphoma compared to other pathologies with lower cellularity, such as radiation necrosis or infarction.^{22,23}

N-acetyl aspartate (NAA, 2.0 ppm) is synthesized from acetylation of the amino acid aspartate in the neuronal mitochondria and is a marker of neuronal viability. Reduction of NAA is seen in many pathologies, such as glioma and radiation necrosis, which involve

destruction or replacement of neurons. Lymphoma or metastases tend to show low or absent NAA levels due to lack of neurons in the tumor component.^{24,25}

Creatine (Cr, 3.0 ppm) has a role in storage and transfer of energy in neurons which have high metabolism. Cr is relatively maintained across a number of disease processes and serves as an internal control which can be used for ratio calculations, such as Cho/Cr.

Lactate (Lac, 1.3 ppm) is a marker of anerobic metabolism and is not seen in normal adult brain spectra due to exclusive aerobic metabolism in brain. Lactate is visualized in necrotic tissues with anerobic metabolism which include abscesses and high grade tumors.^{26,27} Lactate overlaps with lipids at short TE, shows inversion at intermediate TE, and has a characteristic double peak at longer TE²⁸.

Lipids (Lip, 1.3ppm)are components of cell membrane and are increased in diseases with high cell turnover rates such as high grade gliomas. However this is not a specific feature and can be see with other pathologies with high cell turnover/destruction such as abscesses, infarction and metastases.²⁹

Myo-Inositol (MI, 3.5 ppm) is a precursor of phosphatidylinositol (a phospholipid) and of phosphatidylinositol 4,5-bisphosphate. Elevations of MI are seen in low grade gliomas; in contradistinction, reduction seen in WHO grade IV gliomas and can be a useful marker in grading gliomas.³⁰ Elevation of MI can also be seen with other pathologies like dementia of Alzheimer's type and progressive multifocal leukoencephalopathy.

2-Hydroxyglutarate (2-HG, 2.25 ppm) is an oncometabolite of increasing interest in recent times. Tumors with isocitrate dehydrogenase (IDH-1) mutations accumulate higher levels of 2-HG, and as a result detection of 2-HG can be used with reasonable accuracy for non-invasive detection of IDH-1 mutant gliomas.³¹

Other metabolites have been described in the research setting, including metabolites of other nuclei.^{32,33} However, these have demonstrated little clinical importance.

Clinical Relevance – Diagnosis

Years ago, brain tumor work-ups commonly involved a 2-step process including an initial needle biopsy followed by a more definitive surgical resection. The transition to what is usually a single (initial) surgery has been ushered along by developments in neuroimaging, including advanced techniques. MRS is one of those techniques and, along with other methods, this constellation of imaging tools essentially serves as a sort of “virtual biopsy”. In complex cases, such an approach can be used to differentiate gliomas from other diagnoses such as metastases, lymphoma, demyelination, edema, necrosis, and infection. Unfortunately, the spectroscopic profile of high-grade gliomas (HGG) overlaps that of other brain tumors and even non-neoplastic diagnoses on many occasions. It is important to use advanced neuroimaging such as MRS in the context of conventional imaging, including MRI.

Brain metastases, particularly when solitary, can have considerable overlap with the appearance of primary brain tumors on MRI. Both are characterized by enhancing masses with surrounding T2/FLAIR hyperintense edema. Both metastases and gliomas are known to have elevated Cho and decreased NAA compared to adjacent normal white matter. However, lipids and macromolecules are higher in metastases than glioblastoma.³⁴ Evaluating spectroscopic results for the edema next to an enhancing mass may help with diagnosis, as the edema in gliomas more often contains infiltrating tumor cells and as a result has higher Cho/NAA and Cho/Cr.^{24,34-36} As an example of this approach, please see Figure 2. Placement of voxels within the enhancing abnormality is suggestive of a high grade tumor (either glioma or metastasis), but elevated choline in the nonenhancing abnormality is more consistent with a high grade tumor.

Primary central nervous system lymphoma (PCNSL) can also mimic primary brain tumors in many cases. However, there remains some hope for the utility of MRS in these instances. For example, Nagashima et al. recently reported that MI was significantly increased in HGG compared to PCNSL.³⁷ In addition to absolute value measurements, peak ratios have also been used to assist with differentiation. High grade tumors such as lymphoma and HGG have higher elevation of Cho/NAA compared to non-neoplastic diagnoses, such as demyelination.³⁸ While both lymphoma and HGG have Cho/NAA elevation, lymphoma is reported to have lower Cho/NAA than primary brain tumors.³⁹ Figure 3 shows an example of a patient with periventricular abnormality on brain MRI that is most consistent with primary CNS lymphoma on conventional imaging. MR spectroscopy in this setting was consistent with high grade tumor (Figure 3). Spectroscopy does rule out other possibilities such as infection in this case, although this appearance could easily be confused with glioblastoma, highlighting the importance of interpreting MRS alongside conventional imaging. For further review of intracranial lymphoma including MRS see an article by Brandao and Castillo.⁴⁰

Tumefactive demyelinating lesions (TDL) have an overlapping appearance with primary brain tumors. Results have been conflicting regarding the value of MRS in these cases. Ikeguchi et al. found that a Cho/NAA ratio > 1.72 favors HGG over TDL.⁴¹ These results contrast with those of Saindane et al. who found no difference Cho/Cr ratios in contrast-enhancing, central, or perilesional areas of TDLs and gliomas.⁴² TDL are most associated with loss of normal neuronal peaks including Cr and NAA. Figure 4 shows an example of tumefactive demyelination that has a typical appearance on conventional imaging. The MR spectroscopic results are most notable for the presence of prominent lactate and absence of peak ratios suggestive of high grade tumor (Figure 4). In our experience, prominent lactate is rarely associated with untreated brain tumors.

Another type of brain mass which can occasionally be misinterpreted as primary brain tumor is pyogenic brain abscess. The conventional imaging, especially DWI and ADC evaluation of the central non-enhancing material is traditionally quite helpful. As one might imagine, identification of lactate commonly overlaps both entities.⁴³ The classic MRS description of abscess includes presence of amino acid peaks such as valine, alanine, leucine, acetate, succinate.⁴³ However, Pal et al. found that amino acids, while found in 80% of abscesses,

had a sensitivity and specificity of 0.72 and 0.30, respectively.⁴⁴ The clinical utility of numbers like these is unclear at best.

To summarize, a Venn diagram of MRS for astrocytoma/glioma, lymphoma, TDL and brain abscess would not have distinct circles. An individual patient may have an MRS pattern that suggests one of these diagnoses, but this result is best interpreted in the setting of the conventional MR imaging results and the clinical presentation. A combination of peak presence (especially combinations), peak height, area under the (peak) curve and peak ratio may be helpful whereas individual values are challenging to interpret. Future work using MRS as a multiparametric biomarker, including incorporation of machine learning techniques, may increase its ability to differentiate these diagnoses and predict patient prognosis.³⁵ In reviewing the literature, it is clear that the consensus is that there is no consensus.

Clinical Relevance – Tumor grading

MRS has a clinical role in grading gliomas. In conjunction with other imaging features like hemorrhage, necrosis, and enhancement it can be useful to support a diagnosis of high grade glioma vs low grade glioma. Typical abnormal spectroscopic features of low grade gliomas include modest Cho elevation, NAA reduction, and Cho/Cr ratio elevation (Figure 5). MI and MI/Cr ratio can also be elevated. Low grade gliomas typically lack Lac and Lip peaks. In some cases, low grade gliomas may have only mild changes in Cho or NAA with some changes in MI. Therefore, it should be noted that short TE spectroscopy with more detectable metabolites is helpful in low grade gliomas.

High grade gliomas tend to have more dramatic MRS changes compared to low grade tumors. Typical MRS features of grade III and IV gliomas include increased Cho and decreased Cr, NAA, and MI (Figure 2). NAA is seen in higher concentrations in low grade gliomas relative to high grade gliomas and can be used as a marker of prognosis and grading gliomas.⁴⁵ Reductions in Cr can be seen and in combination with increased Cho results in higher Cho/Cr ratios in high grade gliomas compared to low grade gliomas.⁴⁵ There can be variations in spectroscopy abnormalities in glioblastoma depending on the area sampled, and sampling of necrotic regions may show only lipid and lactate peaks with reduced/absent Cho peak. Presence of lactate and lipid peaks suggests a grade IV tumor and is not commonly seen with grade III gliomas.

As there is considerable overlap in spectroscopy patterns of low grade versus high grade gliomas, semi-quantitative analysis using ratios of various metabolites is used to better predict the grade. Commonly used ratios are Cho/Cr, Cho/NAA, NAA/Cr. Typical pattern in high grade gliomas is elevated Cho/Cr, Cho/NAA ratios and reduced NAA/Cr ratio. Cho/Cr is the most commonly used in clinical practice and in research studies. Wang et al, in a large meta-analysis looked at thirty articles comprising 1228 patients and analyzed utility of various metabolite ratios in predicting grade of gliomas and distinguishing low grade gliomas from high grade gliomas.⁴⁶ Quantitative synthesis of studies showed that the pooled sensitivity/specificity of Cho/Cr, Cho/NAA and NAA/Cr ratios was 0.75/0.60, 0.80/0.76 and 0.71/0.70, respectively. The area under the curve (AUC) of the SROC was 0.83, 0.87 and

0.78, respectively. In this analysis all the three ratios had comparable performance and Cho/NAA ratio showed the highest accuracy. However, it should be noted that there was wide variation in the ratio cut offs used in these studies.

Clinical Relevance – Follow-up

MRS can be useful in the longitudinal follow-up of brain tumor patients, particularly for troubleshooting cases in which there may be significant overlap between tumor progression and radiation effects. Worsening in both post-contrast enhancement on T1 weighted imaging and surrounding FLAIR hyperintense edema can both occur because of radiation injury to the tumor and surrounding normal tissue.⁴⁷ Pseudoprogession is the phenomenon of acute imaging worsening in the early phase after radiation, usually within the first 3-6 months after completing chemoradiation.⁴⁸ Pseudoprogession can occur in as many as 20-30% of primary brain tumors and is more common in patients with O6-methylguanine–DNA methyltransferase (MGMT) methylation.⁴⁹ Furthermore, pseudoprogession is associated with improved patient outcomes. It is important to differentiate pseudoprogession from true tumor progression, as tumor progression in this early period would indicate a failure of initial therapy which would necessitate a change in therapy, often taking a patient off the well tolerated and often effective temozolomide to begin another therapy such as lomustine. Interpretation guidelines such as the Response Assessment in Neuro-Oncology (RANO) advise conservative interpretation of cases in the first 3 months after completing radiation, assuming imaging worsening is pseudoprogession as long as they occur in the radiation treatment field.⁵⁰ Pseudoprogession is usually self-limited,⁴⁸ and when imaging does not improve on subsequent follow-up, interpretation is more nuanced and determining if worsening represents tumor progression is more challenging. Radiation necrosis can also occur in a delayed fashion any time from months to years after completing radiation therapy. It can have progressive worsening of enhancement, edema, and mass effect along with worsening patient symptoms. Later radiation necrosis poses a considerable diagnostic dilemma because of its highly variable timing.

Advanced imaging, including MRS, can be a useful tool in differentiating treatment effects from tumor progression, and the imaging appearance of pseudoprogession and delayed radiation necrosis are similar. Radiation results in decreased NAA, Cho, and Cr compared to patients with tumor recurrence.⁴⁷ Using ratios including Cho/Cr can further improve performance of spectroscopy, with higher Cho/Cr in cases of tumor progression. In a meta-analysis of 477 lesions, MRS had moderate performance in differentiating radiation necrosis from glioma recurrence, with Cho/Cr ratio having a sensitivity, specificity, and AUC of 0.83, 0.83, and 0.91, respectively.⁵¹ Compared to progressive tumor, radiation necrosis is also more likely to show elevation in Lip and Lac (Figure 6).⁵²

MRS has performed similar or better than other advanced techniques for evaluating potential radiation necrosis.⁵³ MR perfusion has shown promise in evaluating necrosis, with hyperperfusion associated with tumor recurrence.⁴⁷ Positron emission tomography (PET) with both ¹⁸F-FDG and ¹¹C-methionine, an amino acid tracer, have had intermediate results. Quantitative diffusion imaging has also been relatively promising (sensitivity 75%, specificity 88.9%), with radiation necrosis having greater reduction in central apparent

diffusion coefficient values.⁵⁴ Combined approaches using MRS in conjunction with other advanced imaging may have the best performance.

Limitations

Use of MRS in evaluation and follow up of brain tumors has several significant limitations. The primary limitation is the considerable overlap between the spectroscopic appearance of different pathology. Each pathology has characteristic features that may occur most commonly, but typical diagnostic accuracy may range from 60-80%. However, because of overlapping appearance, many times short term follow-up imaging (4-6 weeks) or surgical biopsy are required to confirm a diagnosis. The lack of definitive imaging findings has been the primary reason MRS is not used more frequently. Other technical limitations also confound implementation of MRS. Imaging sites and scanners vary widely in their implementation, and there is little widespread standardization of imaging techniques. Artifacts and noise are common and further limit interpretation. Susceptibility from adjacent bone or air limit signal from portions of the brain near the skull base and calvarium. Averaging of all signal within relatively large voxels limits evaluation of small lesions, and incomplete water and lipid suppression can completely obscure the diagnostic signal. Imaging can also be time-consuming and require technologist or radiologist intervention. All these limitations are the subject of ongoing research and development.

Future Directions

Research is currently underway to improve current technology and develop new applications to increase the clinical usefulness of MRS in brain tumor diagnosis and treatment. Sequence development is geared towards improving resolution, brain coverage, and speed while decreasing artifacts. Conventional Cartesian 2D or 3D phase-encoding approaches can give excellent quality data, but they rapidly become too time consuming with increasing spatial resolution and brain coverage. A number of methods to accelerate MRS have been described, include parallel imaging and compressed sensing.⁵⁵⁻⁵⁷ Alternative strategies are required to increase acquisition speed by an order of magnitude or more; echo-planar spectroscopic imaging (EPSI) is one of the oldest but also one of the fastest acceleration methods for MRS.⁵⁸⁻⁶¹ In EPSI, k-space is traversed in a rectilinear manner by the oscillating read gradient that is applied simultaneously with spectral data acquisition. For a 3D acquisition, the other two dimensions are encoded using conventional (or elliptical) phase-encoding. Scan times can be reduced even further through under-sampling approaches such as SENSE or GRAPPA in these dimensions.⁶²⁻⁶⁴ When combined with advanced water and lipid suppression techniques, EPSI can be used to obtain high resolution whole brain spectroscopic maps with scan times ranging from 10 to 18 min.^{59,65,66} Smaller voxel sizes result in decreased artifact from surrounding structures and less partial volume artifact. Whole brain coverage further allows novel applications such as biopsy⁶⁷ and treatment planning. These applications are not limited by overlap between different pathology, as the disease of often already known and MRS is being used to define the involved region.

Using MRS to choose optimal biopsy sites is made possible by whole brain spectroscopic imaging. Brain tumors are highly infiltrative, and diagnosis of grade II and III gliomas can be particularly challenging because they are heterogenous tumors that can lack well defined enhancement.⁶⁸ Biopsy is taken from areas of hyperintensity on T2/FLAIR images, but this does not account for areas of tumor heterogeneity and can result in undersampling of high grade or anaplastic areas.⁶⁹⁻⁷¹ Whole brain EPSI can be a useful adjunct to conventional imaging to guide biopsy target selection, with Cho or Cho/NAA maps overlaid on anatomic images and uploaded to surgical guidance software to choose a biopsy site (Figure 7) (manuscript in preparation). Greater metabolite abnormalities are associated with more proliferative areas, and sampling these regions maximizes the chance of sampling high grade areas.^{45,72}

Advanced treatment planning is also a potential application of whole brain MRS.⁷³⁻⁷⁶ In grade IV tumors, high dose radiation is targeted to the resection cavity and areas of residual contrast enhancement which may underrepresent areas of infiltrative tumor.⁷² Recurrence can then occur in surrounding areas undertreated by existing radiation plans. An improved strategy might be to treat areas of greater spectroscopic abnormality, such as those with elevated Cho/NAA ratio, with high dose radiation to the area meeting a threshold difference from normal white matter (Figure 8). A multisite clinical trial recently completed patient enrollment to test this approach (NCT03137888) and is currently in the follow-up period.⁷⁷

Summary

MRS is an advanced technique that allows for molecular evaluation of tissue composition without contrast or radiation. It has a valuable role in the diagnosis, treatment, and subsequent evaluation of brain tumor patients, particularly as a troubleshooting tool when conventional imaging findings of two diagnoses overlap. Unfortunately, overlap between spectroscopy findings and technical limit its accuracy, MRS is most useful when interpreted in conjunction with MRI findings and other advanced techniques. Future developments promise faster and more accurate MRS which can be applied to novel applications such as biopsy and treatment planning.

References

1. Proctor WG, Yu FC. The Dependence of a Nuclear Magnetic Resonance Frequency. *Phys Rev.* 1950;77:717.
2. Julia-Sape M, Candiota AP, Arus C. Cancer metabolism in a snapshot: MRS(I). *NMR Biomed.* 2019;32(10):e4054. [PubMed: 30633389]
3. Ernst RR, Anderson WA. Application of Fourier transform spectroscopy to magnetic resonance. *Rev Sci Instr.* 1966;37:93–102.
4. Ernst RR, Bodenhausen G, Wokaun A. *Principles of Nuclear Magnetic Resonance in One and Two Dimensions Vol 1.* New York, NY: Oxford University Press; 1990.
5. Behar KL, Ogino T. Characterization of macromolecule resonances in the ¹H NMR spectrum of rat brain. *Magn Reson Med.* 1993;30(1):38–44. [PubMed: 8371672]
6. Barker PB, Gillard JH, van Zijl PC, et al. Acute stroke: evaluation with serial proton MR spectroscopic imaging. *Radiology.* 1994;192(3):723–732. [PubMed: 8058940]
7. Lin DD, Crawford TO, Barker PB. Proton MR spectroscopy in the diagnostic evaluation of suspected mitochondrial disease. *AJNR Am J Neuroradiol.* 2003;24(1):33–41. [PubMed: 12533324]

8. Remy C, Grand S, Lai ES, et al. 1H MRS of human brain abscesses in vivo and in vitro. *Magn Reson Med*. 1995;34(4):508–514. [PubMed: 8524016]
9. Luyten PR, den Hollander JA. Observation of metabolites in the human brain by MR spectroscopy. *Radiology*. 1986;161(3):795–798. [PubMed: 3786735]
10. Hanstock CC, Rothman DL, Prichard JW, Jue T, Shulman RG. Spatially localized 1H NMR spectra of metabolites in the human brain. *Proc Natl Acad Sci U S A*. 1988;85(6):1821–1825. [PubMed: 3162309]
11. Bottomley PA, Edelstein WA, Foster TH, Adams WA. In vivo solvent-suppressed localized hydrogen nuclear magnetic resonance spectroscopy: a window to metabolism? *Proc Natl Acad Sci U S A*. 1985;82(7):2148–2152. [PubMed: 3856889]
12. Bax A, Freeman R. Enhanced NMR resolution by restricting the effective sample volume. *J Magn Reson*. 1980;37:177–181.
13. Aue WP. Localization Methods for in vivo NMR Spectroscopy. *Rev Magn Reson Med*. 1986;1:21–72.
14. Frahm J Localized Proton Spectroscopy using stimulated echoes. *J Magn Reson*. 1987;72(3):502–508.
15. Frahm J, Bruhn H, Gyngell ML, Merboldt KD, Hanicke W, Sauter R. Localized high-resolution proton NMR spectroscopy using stimulated echoes: initial applications to human brain in vivo. *Magn Reson Med*. 1989;9(1):79–93. [PubMed: 2540396]
16. Granot J. Selected Volume Excitation Using Stimulated Echoes (VEST). Applications to spatially localized spectroscopy and imaging. *J Magn Reson*. 1986;70(3):488–492.
17. Kimmich R, Hoepfel D. Volume-selective multipulse spin-echo spectroscopy. *J Magn Reson*. 1987;72(2):379–384.
18. Bottomley PA, Inventor; General Electric Company, assignee. Selective volume method for performing localized NMR spectroscopy. US patent 4480228. 10 30th 1984, 1984.
19. Ordidge RJ, Gordon RE, Inventors; Oxford Research Systems Limited, assignee. Methods and apparatus of obtaining NMR spectra. US patent 45310941983.
20. van Zijl PC, Moonen CT, Alger JR, Cohen JS, Chesnick SA. High field localized proton spectroscopy in small volumes: greatly improved localization and shimming using shielded strong gradients. *Magn Reson Med*. 1989;10(2):256–265. [PubMed: 2548056]
21. Nelson SJ. Analysis of volume MRI and MR spectroscopic imaging data for the evaluation of patients with brain tumors. *Magn Reson Med*. 2001;46(2):228–239. [PubMed: 11477625]
22. Brandão LA, Castillo M. Adult Brain Tumors: Clinical Applications of Magnetic Resonance Spectroscopy. *Magn Reson Imaging Clin N Am*. 2016;24(4):781–809. [PubMed: 27742117]
23. Shimizu H, Kumabe T, Shirane R, Yoshimoto T. Correlation between choline level measured by proton MR spectroscopy and Ki-67 labeling index in gliomas. *AJNR Am J Neuroradiol*. 2000;21(4):659–665. [PubMed: 10782774]
24. Server A, Josefsen R, Kulle B, et al. Proton magnetic resonance spectroscopy in the distinction of high-grade cerebral gliomas from single metastatic brain tumors. *Acta Radiol*. 2010;51(3):316–325. [PubMed: 20092374]
25. Chen L, Du P, Guo Z, Mao W, Cao A. Diagnosis of Intracranial Primary Central Nervous System Lymphoma Based on Magnetic Resonance Imaging. *Neurosci Lett*. 2020:135225. [PubMed: 32619655]
26. Fan G. Comments and controversies: magnetic resonance spectroscopy and gliomas. *Cancer Imaging*. 2006;6:113–115. [PubMed: 16966066]
27. Lai PH, Ho JT, Chen WL, et al. Brain abscess and necrotic brain tumor: discrimination with proton MR spectroscopy and diffusion-weighted imaging. *AJNR Am J Neuroradiol*. 2002;23(8):1369–1377. [PubMed: 12223380]
28. Yamasaki F, Takaba J, Ohtaki M, et al. Detection and differentiation of lactate and lipids by single-voxel proton MR spectroscopy. *Neurosurg Rev*. 2005;28(4):267–277. [PubMed: 16133454]
29. Brandão LA, Castillo M. Adult brain tumors: clinical applications of magnetic resonance spectroscopy. *Neuroimaging Clin N Am*. 2013;23(3):527–555. [PubMed: 23928203]

30. Castillo M, Smith JK, Kwock L. Correlation of myo-inositol levels and grading of cerebral astrocytomas. *AJNR Am J Neuroradiol.* 2000;21(9):1645–1649. [PubMed: 11039343]
31. Suh CH, Kim HS, Jung SC, Choi CG, Kim SJ. Imaging prediction of isocitrate dehydrogenase (IDH) mutation in patients with glioma: a systemic review and meta-analysis. *Eur Radiol.* 2019;29(2):745–758. [PubMed: 30003316]
32. Grist JT, Miller JJ, Zaccagna F, et al. Hyperpolarized (13)C MRI: A novel approach for probing cerebral metabolism in health and neurological disease. *J Cereb Blood Flow Metab.* 2020;40(6):1137–1147. [PubMed: 32153235]
33. Wenger KJ, Hattingen E, Franz K, Steinbach J, Bahr O, Pilatus U. In vivo Metabolic Profiles as Determined by (31)P and short TE (1)H MR-Spectroscopy : No Difference Between Patients with IDH Wildtype and IDH Mutant Gliomas. *Clin Neuroradiol.* 2019;29(1):27–36. [PubMed: 28983683]
34. Pope WB. Brain metastases: neuroimaging. *Handb Clin Neurol.* 2018;149:89–112. [PubMed: 29307364]
35. Durmo F, Rydelius A, Cuellar Baena S, et al. Multivoxel (1)H-MR Spectroscopy Biometrics for Preoperative Differentiation Between Brain Tumors. *Tomography.* 2018;4(4):172–181. [PubMed: 30588503]
36. Chiang IC, Kuo YT, Lu CY, et al. Distinction between high-grade gliomas and solitary metastases using peritumoral 3-T magnetic resonance spectroscopy, diffusion, and perfusion imagings. *Neuroradiology.* 2004;46(8):619–627. [PubMed: 15243726]
37. Nagashima H, Sasayama T, Tanaka K, et al. Myo-inositol concentration in MR spectroscopy for differentiating high grade glioma from primary central nervous system lymphoma. *J Neurooncol.* 2018;136(2):317–326. [PubMed: 29143277]
38. Lu SS, Kim SJ, Kim HS, et al. Utility of proton MR spectroscopy for differentiating typical and atypical primary central nervous system lymphomas from tumefactive demyelinating lesions. *AJNR Am J Neuroradiol.* 2014;35(2):270–277. [PubMed: 23928144]
39. Vallee A, Guillevin C, Wager M, Delwail V, Guillevin R, Vallee JN. Added Value of Spectroscopy to Perfusion MRI in the Differential Diagnostic Performance of Common Malignant Brain Tumors. *AJNR Am J Neuroradiol.* 2018;39(8):1423–1431. [PubMed: 30049719]
40. Brandao LA, Castillo M. Lymphomas-Part 1. *Neuroimaging Clin N Am.* 2016;26(4):511–536. [PubMed: 27712792]
41. Ikeguchi R, Shimizu Y, Abe K, et al. Proton magnetic resonance spectroscopy differentiates tumefactive demyelinating lesions from gliomas. *Mult Scler Relat Disord.* 2018;26:77–84. [PubMed: 30237108]
42. Saindane AM, Cha S, Law M, Xue X, Knopp EA, Zagzag D. Proton MR spectroscopy of tumefactive demyelinating lesions. *AJNR Am J Neuroradiol.* 2002;23(8):1378–1386. [PubMed: 12223381]
43. Kim SH, Chang KH, Song IC, et al. Brain abscess and brain tumor: discrimination with in vivo H-1 MR spectroscopy. *Radiology.* 1997;204(1):239–245. [PubMed: 9205254]
44. Pal D, Bhattacharyya A, Husain M, Prasad KN, Pandey CM, Gupta RK. In vivo proton MR spectroscopy evaluation of pyogenic brain abscesses: a report of 194 cases. *AJNR Am J Neuroradiol.* 2010;31(2):360–366. [PubMed: 19797788]
45. Bulik M, Jancalék R, Vanicek J, Skoch A, Mechl M. Potential of MR spectroscopy for assessment of glioma grading. *Clin Neurol Neurosurg.* 2013;115(2):146–153. [PubMed: 23237636]
46. Wang Q, Zhang H, Zhang J, et al. The diagnostic performance of magnetic resonance spectroscopy in differentiating high-from low-grade gliomas: A systematic review and meta-analysis. *Eur Radiol.* 2016;26(8):2670–2684. [PubMed: 26471274]
47. Siu A, Wind JJ, Iorgulescu JB, Chan TA, Yamada Y, Sherman JH. Radiation necrosis following treatment of high grade glioma--a review of the literature and current understanding. *Acta Neurochir (Wien).* 2012;154(2):191–201; discussion 201. [PubMed: 22130634]
48. Parvez K, Parvez A, Zadeh G. The diagnosis and treatment of pseudoprogression, radiation necrosis and brain tumor recurrence. *Int J Mol Sci.* 2014;15(7):11832–11846. [PubMed: 24995696]

49. Brandes AA, Franceschi E, Tosoni A, et al. MGMT promoter methylation status can predict the incidence and outcome of pseudoprogression after concomitant radiochemotherapy in newly diagnosed glioblastoma patients. *J Clin Oncol*. 2008;26(13):2192–2197. [PubMed: 18445844]
50. Wen PY, Macdonald DR, Reardon DA, et al. Updated response assessment criteria for high-grade gliomas: response assessment in neuro-oncology working group. *J Clin Oncol*. 2010;28(11):1963–1972. [PubMed: 20231676]
51. Zhang H, Ma L, Wang Q, Zheng X, Wu C, Xu BN. Role of magnetic resonance spectroscopy for the differentiation of recurrent glioma from radiation necrosis: a systematic review and meta-analysis. *Eur J Radiol*. 2014;83(12):2181–2189. [PubMed: 25452098]
52. Nakajima T, Kumabe T, Kanamori M, et al. Differential diagnosis between radiation necrosis and glioma progression using sequential proton magnetic resonance spectroscopy and methionine positron emission tomography. *Neurol Med Chir (Tokyo)*. 2009;49(9):394–401. [PubMed: 19779283]
53. van Dijken BRJ, van Laar PJ, Holtman GA, van der Hoorn A. Diagnostic accuracy of magnetic resonance imaging techniques for treatment response evaluation in patients with high-grade glioma, a systematic review and meta-analysis. *Eur Radiol*. 2017;27(10):4129–4144. [PubMed: 28332014]
54. Zakhari N, Taccone MS, Torres C, et al. Diagnostic Accuracy of Centrally Restricted Diffusion in the Differentiation of Treatment-Related Necrosis from Tumor Recurrence in High-Grade Gliomas. *AJNR Am J Neuroradiol*. 2018;39(2):260–264. [PubMed: 29217742]
55. Nassirpour S, Chang P, Avdievitch N, Henning A. Compressed sensing for high-resolution nonlipid suppressed (1) H FID MRSI of the human brain at 9.4T. *Magn Reson Med*. 2018;80(6):2311–2325. [PubMed: 29707804]
56. Strasser B, Povazan M, Hangel G, et al. (2 + 1)D-CAIPIRINHA accelerated MR spectroscopic imaging of the brain at 7T. *Magn Reson Med*. 2017;78(2):429–440. [PubMed: 27548836]
57. Thomas MA, Nagarajan R, Huda A, et al. Multidimensional MR spectroscopic imaging of prostate cancer in vivo. *NMR Biomed*. 2014;27(1):53–66. [PubMed: 23904127]
58. Ebel A, Soher BJ, Maudsley AA. Assessment of 3D proton MR echo-planar spectroscopic imaging using automated spectral analysis. *Magn Reson Med*. 2001;46(6):1072–1078. [PubMed: 11746571]
59. Ebel A, Maudsley AA. Improved spectral quality for 3D MR spectroscopic imaging using a high spatial resolution acquisition strategy. *Magn Reson Imaging*. 2003;21(2):113–120. [PubMed: 12670597]
60. Mansfield P Spatial mapping of chemical shift in NMR. *Magn Reson Med*. 1984;1:370–386. [PubMed: 6571566]
61. Posse S, Cuenod CA, Risinger R, Le Bihan D, Balaban RS. Anomalous transverse relaxation in 1H spectroscopy in human brain at 4 Tesla. *Magn Reson Med*. 1995;33(2):246–252. [PubMed: 7707916]
62. Lin FH, Tsai SY, Otazo R, et al. Sensitivity-encoded (SENSE) proton echo-planar spectroscopic imaging (PEPSI) in the human brain. *Magn Reson Med*. 2007;57(2):249–257. [PubMed: 17260356]
63. Tsai SY, Otazo R, Posse S, et al. Accelerated proton echo planar spectroscopic imaging (PEPSI) using GRAPPA with a 32-channel phased-array coil. *Magn Reson Med*. 2008;59(5):989–998. [PubMed: 18429025]
64. Zhu X, Ebel A, Ji JX, Schuff N. Spectral phase-corrected GRAPPA reconstruction of three-dimensional echo-planar spectroscopic imaging (3D-EPSI). *Magn Reson Med*. 2007;57(5):815–820. [PubMed: 17457872]
65. Ebel A, Maudsley AA. Comparison of methods for reduction of lipid contamination for in vivo proton MR spectroscopic imaging of the brain. *Magn Reson Med*. 2001;46(4):706–712. [PubMed: 11590647]
66. Nelson SJ, Li Y, Lupo JM, et al. Serial analysis of 3D H-1 MRSI for patients with newly diagnosed GBM treated with combination therapy that includes bevacizumab. *J Neurooncol*. 2016;130(1):171–179. [PubMed: 27535746]

67. Jin T, Ren Y, Zhang H, Xie Q, Yao Z, Feng X. Application of MRS- and ASL-guided navigation for biopsy of intracranial tumors. *Acta Radiol.* 2019;60(3):374–381. [PubMed: 29958510]
68. Scott JN, Brasher PM, Sevick RJ, Rewcastle NB, Forsyth PA. How often are nonenhancing supratentorial gliomas malignant? A population study. *Neurology.* 2002;59(6):947–949. [PubMed: 12297589]
69. Henson JW, Gaviani P, Gonzalez RG. MRI in treatment of adult gliomas. *Lancet Oncol.* 2005;6(3):167–175. [PubMed: 15737833]
70. Jacobs AH, Kracht LW, Gossmann A, et al. Imaging in neurooncology. *NeuroRx.* 2005;2(2):333–347. [PubMed: 15897954]
71. Weber MA, Giesel FL, Stieltjes B. MRI for identification of progression in brain tumors: from morphology to function. *Expert Rev Neurother.* 2008;8(10):1507–1525. [PubMed: 18928344]
72. Cordova JS, Shu HK, Liang Z, et al. Whole-brain spectroscopic MRI biomarkers identify infiltrating margins in glioblastoma patients. *Neuro Oncol.* 2016;18(8):1180–1189. [PubMed: 26984746]
73. Nelson SJ, Graves E, Pirzkall A, et al. In vivo molecular imaging for planning radiation therapy of gliomas: an application of 1H MRSI. *J Magn Reson Imaging.* 2002;16(4):464–476. [PubMed: 12353260]
74. Pirzkall A, McKnight TR, Graves EE, et al. MR-spectroscopy guided target delineation for high-grade gliomas. *Int J Radiat Oncol Biol Phys.* 2001;50(4):915–928. [PubMed: 11429219]
75. Ken S, Vieilleveigne L, Franceries X, et al. Integration method of 3D MR spectroscopy into treatment planning system for glioblastoma IMRT dose painting with integrated simultaneous boost. *Radiat Oncol.* 2013;8:1. [PubMed: 23280007]
76. Cordova JS, Kandula S, Gurbani S, et al. Simulating the Effect of Spectroscopic MRI as a Metric for Radiation Therapy Planning in Patients with Glioblastoma. *Tomography.* 2016;2(4):366–373. [PubMed: 28105468]
77. Gurbani S, Weinberg B, Cooper L, et al. The Brain Imaging Collaboration Suite (BrICS): A Cloud Platform for Integrating Whole-Brain Spectroscopic MRI into the Radiation Therapy Planning Workflow. *Tomography.* 2019;5(1):184–191. [PubMed: 30854456]

Synopsis

Magnetic resonance spectroscopy (MRS) is a valuable tool for imaging brain tumors, primarily as an adjunct to conventional imaging and clinical presentation. MRS can be useful in initial diagnosis of brain tumors, helping differentiate tumors from possible mimics such as metastatic disease, lymphoma, demyelination, and infection, as well as in the subsequent follow-up of patients after resection and chemoradiation. Unfortunately, the spectroscopic appearance of many pathologies can overlap, and ultimately follow up or biopsy may be required to make a definitive diagnosis. Future developments may continue to increase the value of MRS for initial diagnosis, treatment planning, and early detection of recurrence.

Author Manuscript

Author Manuscript

Author Manuscript

Author Manuscript

Clinics Care Points

- Magnetic resonance spectroscopy (MRS) is an advanced MRI technique that allows non-invasive evaluation of tissue molecular composition.
- High grade neoplasms, including brain tumors, have elevation of choline (Cho), a marker of cell membrane turnover, with decrease in N-acetyl aspartate (NAA), a marker of neuronal integrity.
- The most frequent applications of MRS in brain tumor care are differentiating tumor from other non-neoplastic pathology, estimating tumor grade, and differentiating tumor recurrence from radiation effects.
- Many pathologies overlap in spectroscopic appearance and MRS is best interpreted in conjunction with other imaging findings and clinical considerations.
- Future developments may make whole brain spectroscopic imaging a useful tool for prognostication and treatment planning.

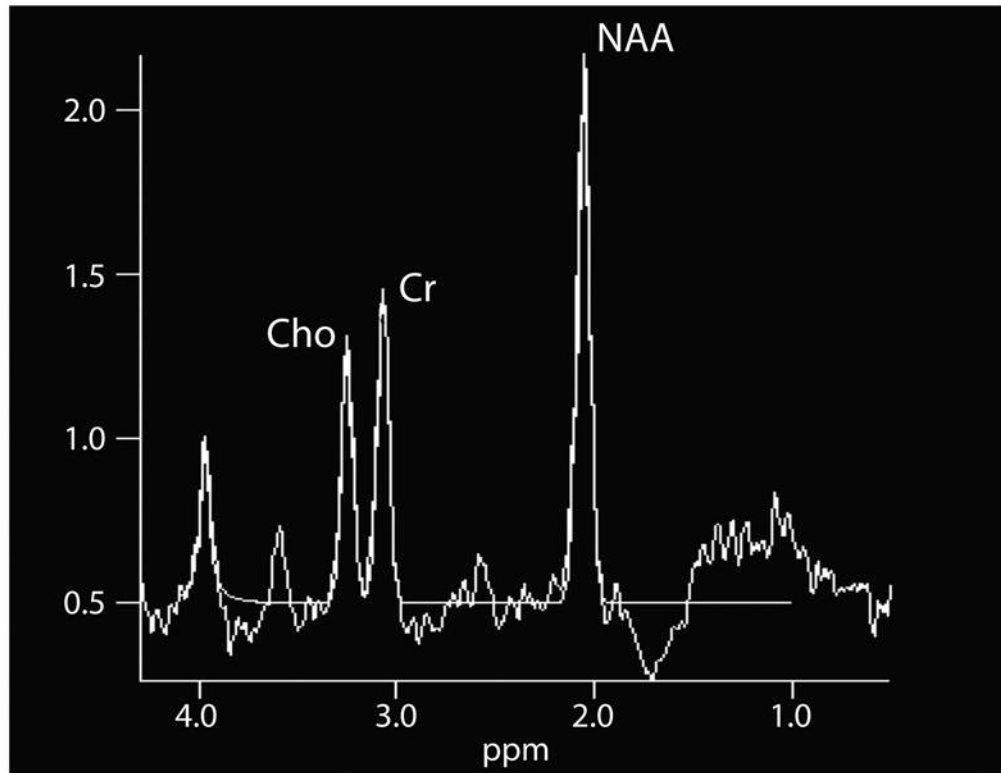


Figure 1. MRS spectrum from an area of normal brain. Choline (Cho), creatine (Cr), and N-acetyl-aspartate (NAA) are the dominant peaks, with NAA higher than both Cho and Cr.

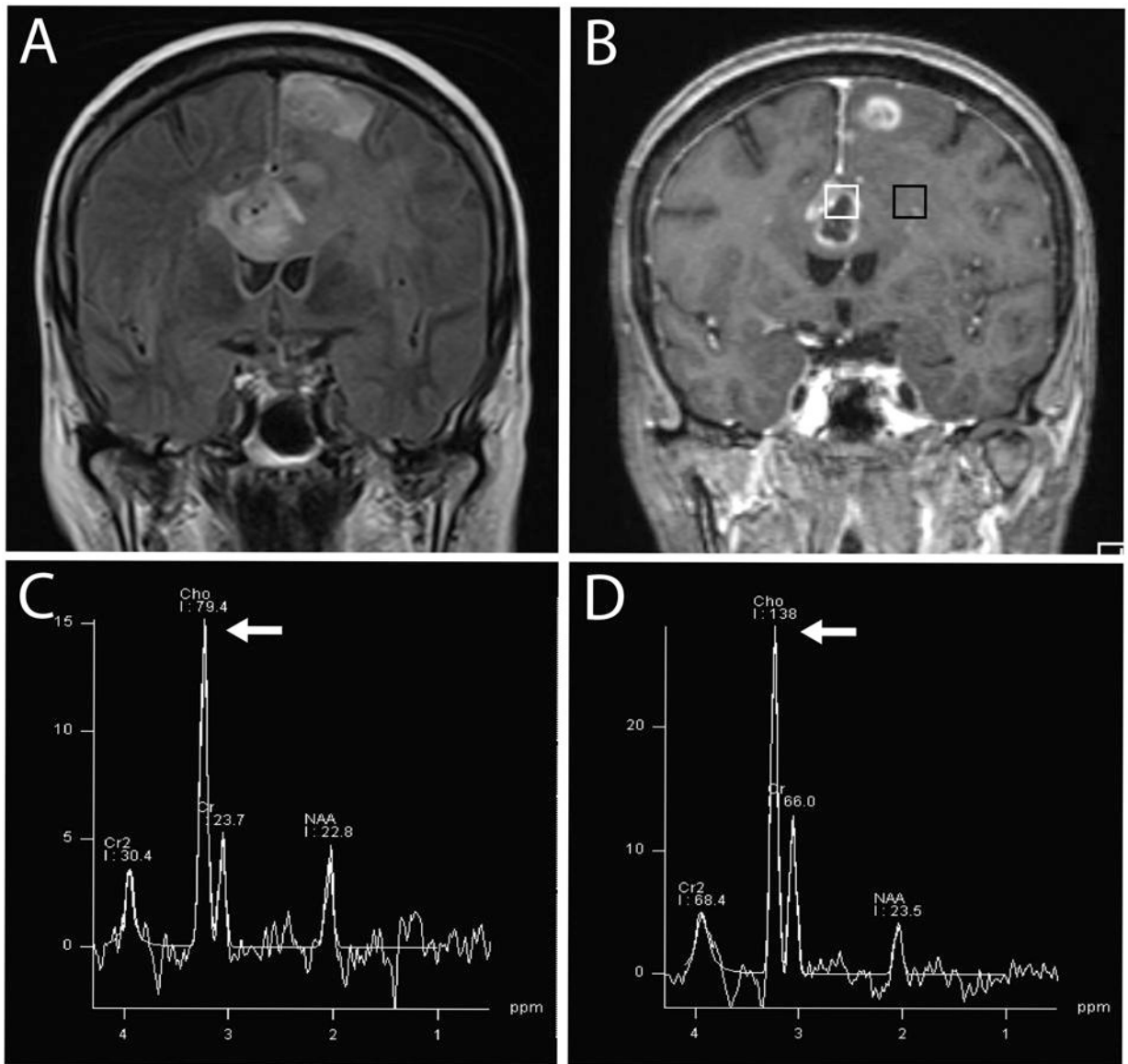


Figure 2.

Glioblastoma. 86 year-old woman with new neurologic symptoms. Coronal FLAIR (A) and contrast enhanced T1 weighted images (B) demonstrate a mass in the corpus callosum and left superior frontal gyrus with multiple areas of enhancement. Spectroscopy (TE 144 ms) from the corpus callosum (C, region of white box in B) shows markedly elevated Cho (white arrow) and relatively low NAA. Spectroscopy from the area of non-enhancing tumor in the left centrum semiovale (D, black box in B) shows similar findings in the non-enhancing areas, confirming infiltrative tumor.

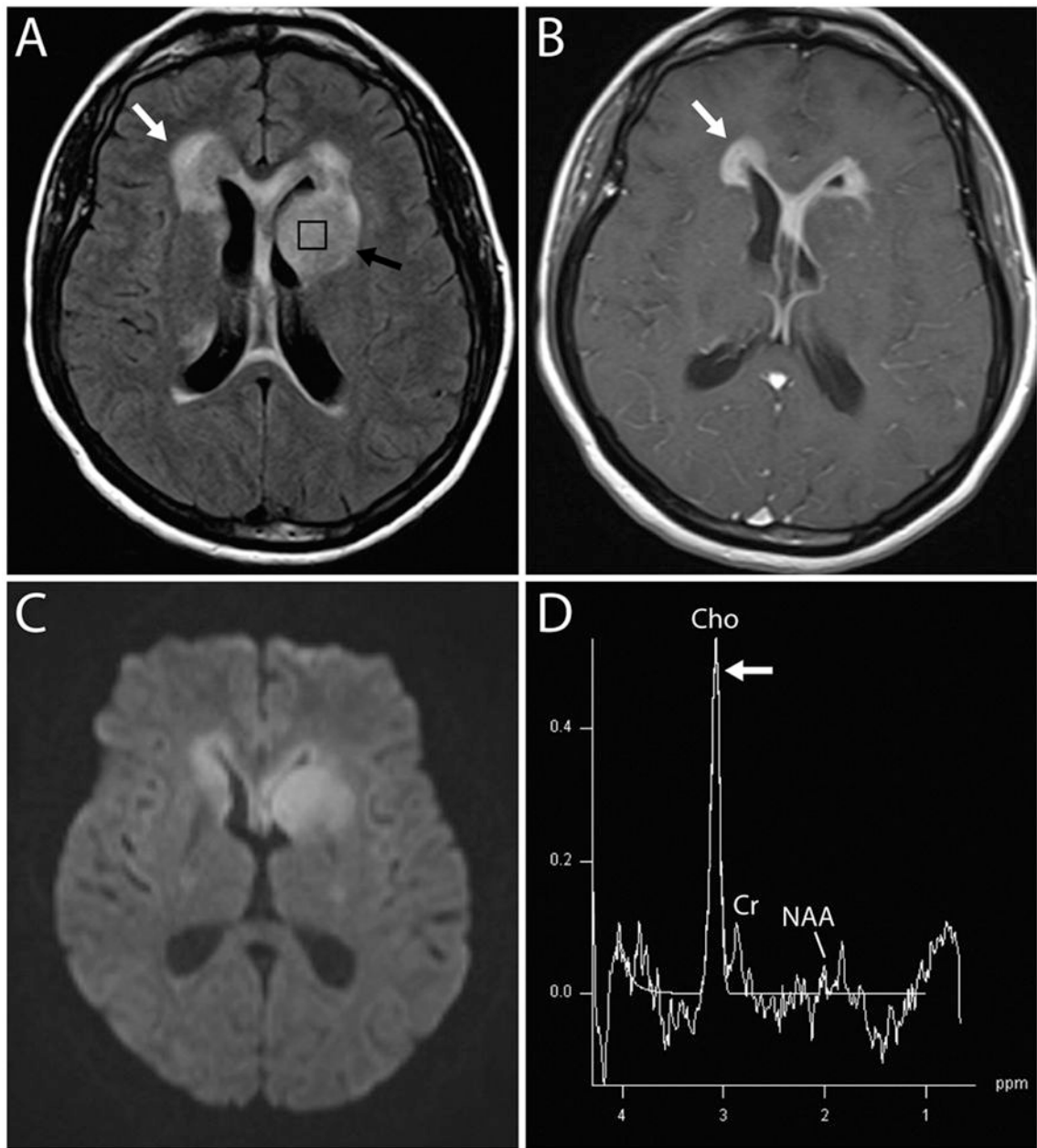


Figure 3. Lymphoma. 40 year-old woman with HIV presented with altered mental status. FLAIR (A) though the basal ganglia showed masslike FLAIR hyperintensity and expansion of the left caudate (black arrow) with multiple periventricular masses which enhance on postcontrast T1 weighted images (B, white arrows). DWI (C) demonstrates associated hyperintensity. Spectroscopy (TE 140 ms) from the caudate (black box, A) shows markedly elevated Cho (white arrow) with very low Cr and NAA.

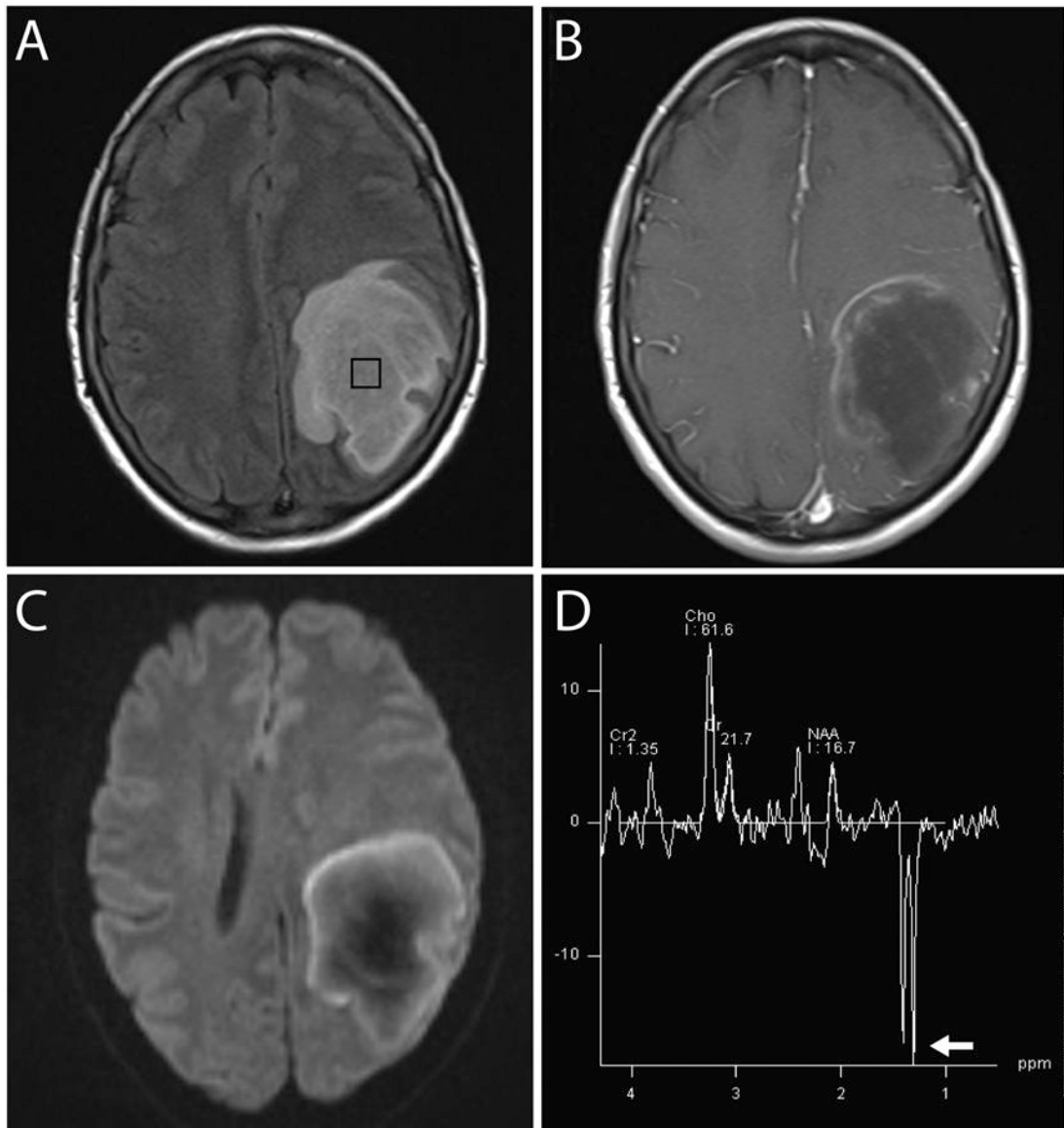


Figure 4. Tumefactive demyelination. 50 year-old woman with right sided weakness. FLAIR (A) images show an expansile, FLAIR hyperintense mass in the left parietal lobe with a peripheral incomplete rim of enhancement on T1 weighted imaging (B). Diffusion weighted imaging (C) similarly shows a peripheral rim of abnormally hyperintense DWI. Spectroscopy (TE 135 ms) (D) from the central portion of the lesion (black box, A) shows elevated Cho, near complete loss of NAA, and a characteristic inverted doublet lactate peak at 1.3 ppm.

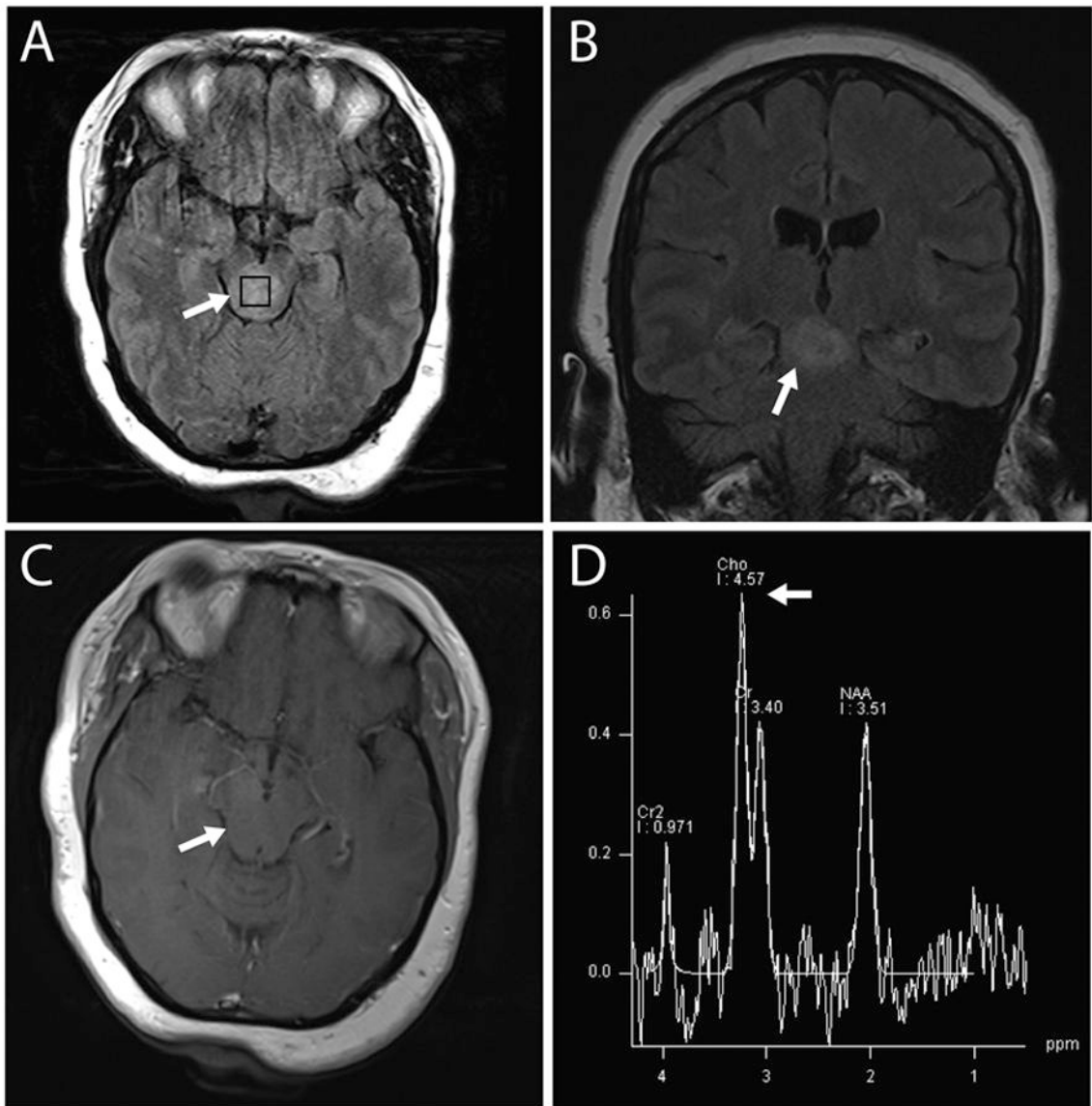


Figure 5.

Low grade glioma. 34 year-old woman with neurofibromatosis type 1. Axial (A) and coronal (B) FLAIR images show an expansile mass within the midbrain with no enhancement on post-contrast T1 weighted images (C) (arrows). Spectroscopy (TE 135 ms) within the midbrain shows modest elevation of Cho (arrow) and depression of NAA. Spectroscopy is particularly important in this difficult to biopsy location.

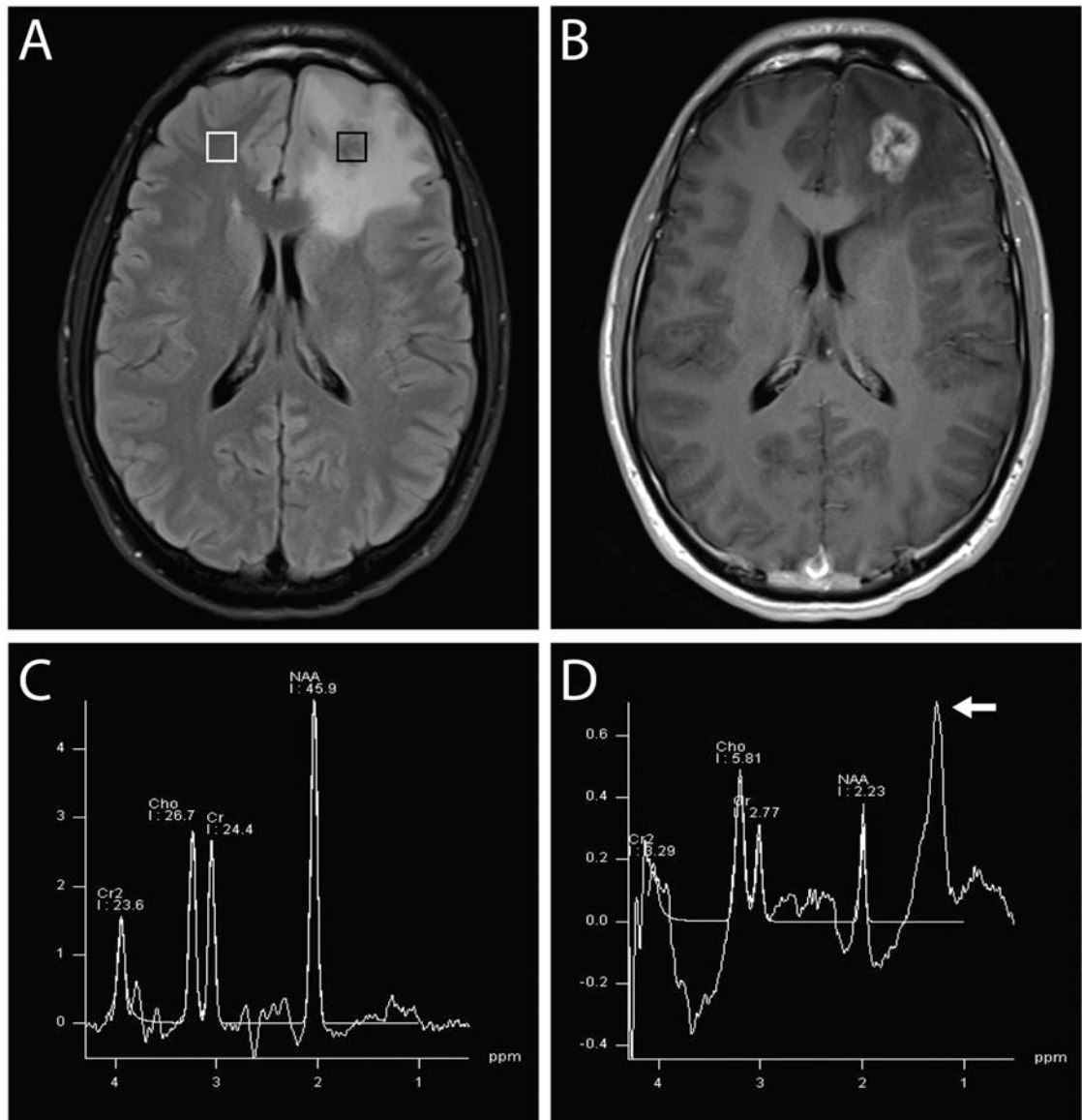


Figure 6. Radiation necrosis. 21 year-old with Ewing sarcoma metastasis to the left frontal lobe previously treated with radiation. Expansile mass in the left frontal lobe with surrounding abnormal FLAIR (A) and central enhancement on post-contrast T1 (B). Spectroscopy (TE 135 ms) of the contralateral normal white matter (C, from white box in A) shows relatively normal spectrum. Spectroscopy of the abnormal region (D, from black box in A) shows decrease in height of all peaks, particularly NAA, with a lipid/lactate peak at 1.3 ppm (white arrow).

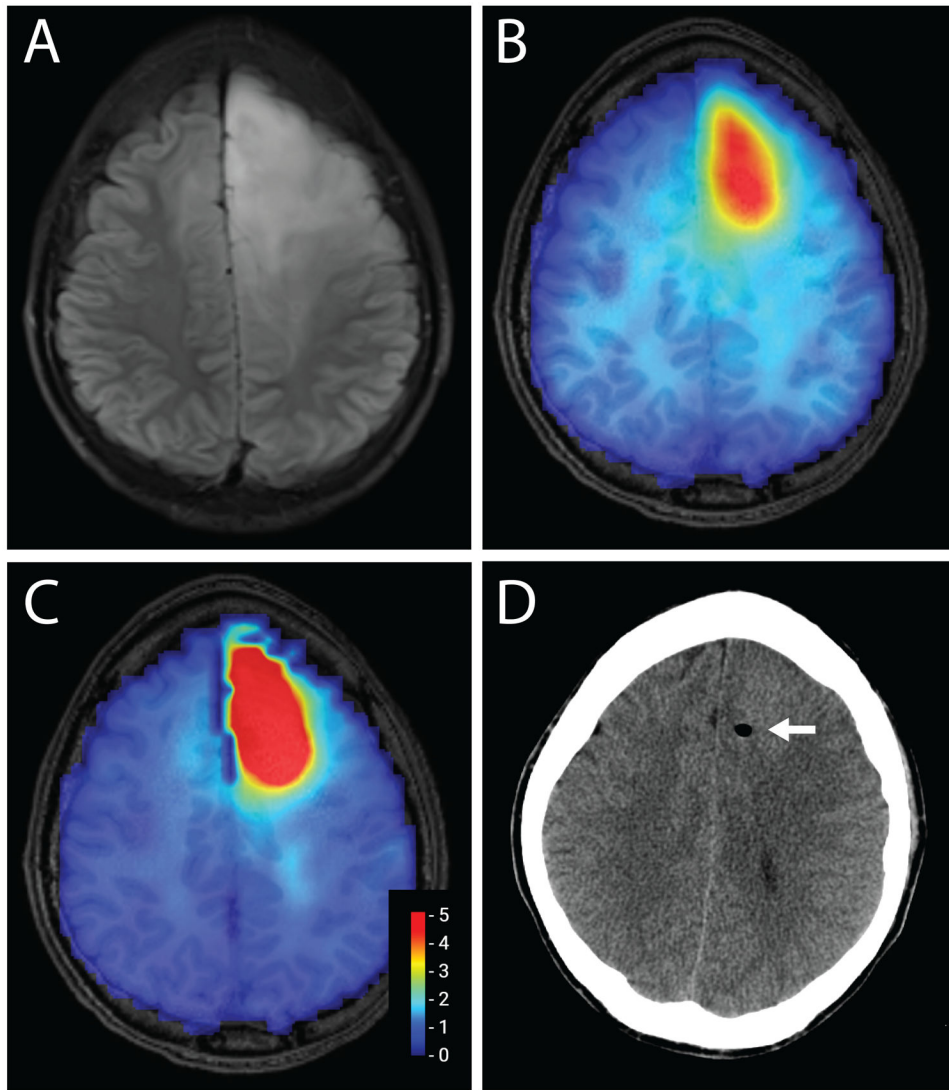


Figure 7. Grade 3 astrocytoma. 31 year-old man with a left frontal expansile, non-enhancing mass seen on FLAIR (A). T1-weighted images overlaid with 3D Cho map (B) and Cho/NAA ratio (C), showing areas of greatest metabolic abnormality. Scale in (C) shows the ratio between Cho/NAA and normal white matter. Stereotactic biopsy was targeted to a region with maximal metabolic abnormality, as seen on post-biopsy CT (D).

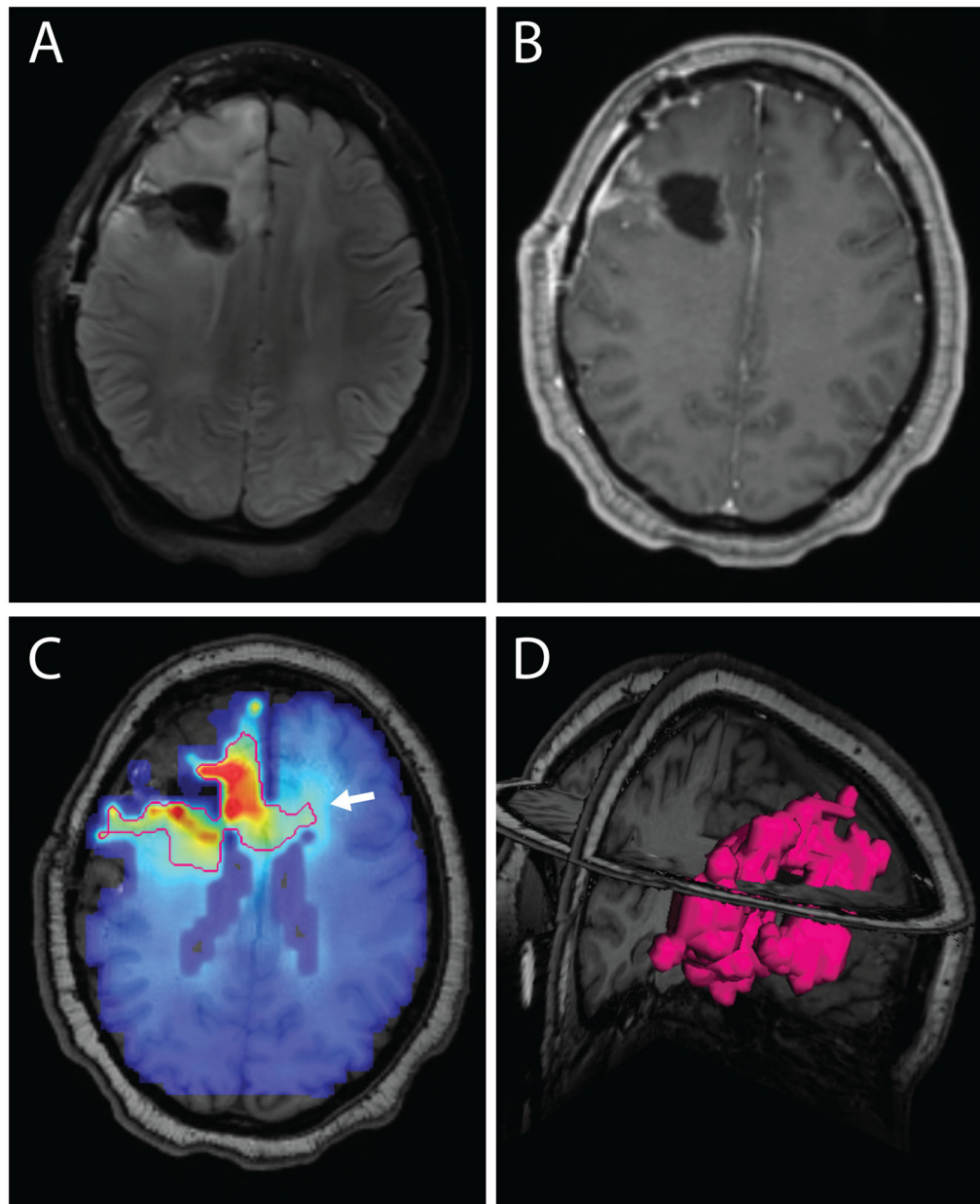


Figure 8.

Glioblastoma. Right frontal glioblastoma, status post resection. FLAIR abnormality surrounds the cavity in the right middle and superior frontal gyri (A). A small amount of nodular enhancement is present around the cavity on postcontrast T1 weighted imaging (B). T1-weighted images overlaid with 3D Cho/NAA ratio (C) shows tumor extending beyond the area of abnormal enhancement and FLAIR (white arrow). The red line outlines the area with a Cho/NAA ratio 2x normal white matter, a threshold associated with 30% tumor in previous biopsy studies. 3-D rendering of area of MRS abnormality surrounding the resection cavity (D).

Table 1.

Potential uses of magnetic resonance spectroscopy in brain tumor imaging

Clinical applications	Research applications
Differentiating tumor from potential mimics Metastatic disease Demyelinating disease Lymphoma Infection Evaluation of treated tumor to differentiate Recurrent tumor Pseudoprogression/radiation necrosis	Three-dimensional evaluation of tumor heterogeneity Detection of molecular/genetic features IDH mutation Treatment planning Surgical resection/biopsy Radiation therapy

Author Manuscript

Author Manuscript

Author Manuscript

Author Manuscript

Table 2.

Frequently encountered metabolites and their characteristics and clinical role in evaluating brain tumors

Metabolite	ppm	Elevated in	Decreased in	<u>Clinical significance in brain tumor imaging</u>
Choline	3.2ppm	Neoplasms Inflammation Gliosis	Necrosis	Grading gliomas Distinguishing glioblastomas for metastases Radiation planning in gliomas Differentiating tumor progression versus pseudo-progression/ Radionecrosis
N-acetyl aspartate	2.0 ppm		Gliomas and more so in high grade gliomas Radiation necrosis Metastases Lymphoma	Grading of gliomas Distinguishing gliomas from metastases
Creatine	3.0 ppm		High grade gliomas Necrosis	Grading of gliomas Distinguishing metastases from Glioblastoma
Lactate	1.3 ppm	Glioblastoma Abscesses	Not present in normal spectra	Grading of gliomas
Lipids	1.3 ppm with inversion at intermediate TE	Glioblastoma Abscess Lymphoma Metastases		Grading of gliomas
Myo-Inositol	3.5 ppm	Low grade gliomas Progressive multifocal encephalopathy	High grade gliomas	Grading of gliomas
2-Hydroxyglutarate	2.5ppm	IDH-1 positive tumors		Detection of IDH-1 positive tumors